

Experimental and finite element analysis of soft nanopillars for biomedical applications*

G Mallikarjunachari *

Department of Mechanical Engineering, Madanapalle Institute of Technology and Science, Madanapalle, Andhra Pradesh

*Presented in 1st National Conference on Smart Manufacturing & Industry 4.0 (NCSMI4) at Central Manufacturing Technology Institute (CMTI), Bengaluru, during May 30-31, 2019.

ABSTRACT

Keywords:

Ball Indentation,
Hyperplastic Membranes,
Nanopillars, and
Young's Modulus

The main objectives of this work are i) synthesise low aspect ratio soft nanopillars of the non-uniform cross-sectional area (tapered) on a polymeric substrate and ii) Design of soft nanopillars applying finite element technique. In this work, the nano-pillars are developed on a flat elastomeric substrate using well-established ball indentation technique. Soft elastomeric nanopillars of height ranging from 50 nm to 500 nm are prepared. Finite element simulations are performed to understand the large deformation behaviour of the elastomer. Different parameters such as indenter diameter, the shape of the indenter and elastomer properties are considered to tune the nanopillar height and width. These high aspect ratio nanopillars on flat surfaces can find many potential applications in recent days. In particular, these nano-pillar surfaces can be efficiently applied in the biomedical fields such as cell mechanics studies and biosensors. In these studies, nanopillar devices are implemented as a means to study cell-substrate, and cell to cell interactions. The stiffness and the deflection characteristics of these nanopillars are extremely necessary for biomedical applications.

1. Introduction

Synthesis and characterization of nanostructured surfaces are gaining significant attention in recent days due to their diversity of applications. Primary applications of these nanostructured surfaces include energy storage [1–3], adhesion [4–6], surface de-wetting [7] and organic solar cells [8,9]. In general, the shape of these nanostructured materials is limited to a particular shape, mostly cylindrical shape [10] with a high aspect ratio [11]. The typical aspect ratio of these micro and nanopillars varies from 20-60 [12]. There are various fabrication techniques such as focused ion beam method [13-14] and micromachining [15] to synthesize the cylindrical shape micro and nanopillars. However, it is extremely challenging to tuning the shape and aspect ratio of these micro and nanopillars using conventional techniques [16-17].

Irrespective of the application, the performance of these soft pillars significantly depends on the mechanical properties such as compression strength [4, 18], bending stiffness [19], and fracture

properties [20]. This mechanical property not only depends on the intrinsic properties of polymers, but properties also depend on the various other parameters. These parameters include the concentration of filler material [21–23], the interaction between the matrix and particles, and particle-particle interactions [24].

In this research work, the application of nanoindentation lithography for creating low aspect ratio soft nanopillars is proposed. The height and width of the pillar was controlled by changing the concentration of the filler (clay) material and magnitude of the load.

2. Materials and Methods

The materials Polymethylmethacrylate (PMMA), clay and silicone elastomer are used in this study. Different material systems are prepared by changing the concentration of clay in both PMMA and silicone elastomer. Table 1 presents the materials used in this study. The materials system 1, 3, 4, and 5 are synthesized using solvent casting method. Moreover, the material systems 2, 6, 7 and 8 are synthesized using room temperature curing method. The nanoindentation experiments were conducted using the

*Corresponding author,
E-mail: drmallikarjunacharig@mits.ac.in(Mallikarjunachari G)

$$H = \frac{P}{A_c} \dots (1a) \quad A_c = f(h_c) = C_1 h_c^2 + C_2 h_c + C_3 h_c^{1/2} + C_4 h_c^{1/4} \dots (1b) \quad E_r = \frac{\sqrt{\pi}}{2\beta} \frac{s}{\sqrt{A_c}} \quad (1c) \dots (1)$$

Berkovich indenter (Bruker Hysitron TI premier) with diamond tip (Young’s modulus (E) = 1140 GPa, Poisson’s ratio (ν) = 0.07). Appropriate load function (loading 20 sec), (holding 10 sec and unloading 10 sec) was used for all the

samples [41]. The hardness (H) and Young’s modulus (E_r) were obtained as a function of load (or penetration depth) given by equations (1a-1c) and are directly obtained from the instrument. Where, P is the maximum load, C_1, C_2, C_3, C_4 and β are the constants, and E_r is the reduced Young’s modulus as expressed in equation 1c. Different sets of peak loads ranging from 20 μN to 7000 μN were applied depending upon the thin film-substrate material systems.

Table 1
Material systems used in the current study.

| S. No. | Matrix Material | Filler Material | Concentration |
|--------|--------------------|-----------------|---------------|
| 1 | PMMA | None | None |
| 2 | Silicone Elastomer | None | None |
| 3 | PMMA | Clay | 1% |
| 4 | PMMA | Clay | %5 |
| 5 | PMMA | Clay | %10 |
| 6 | Silicone Elastomer | Clay | %1 |
| 7 | Silicone Elastomer | Clay | %5 |
| 8 | Silicone Elastomer | Clay | 10% |

3. Result and Discussions

Depth control nanoindentation experiments are conducted on the materials systems PMMA, and its composites. Different shape indenters three-sided (Berkovich) and conical shape are used for the indentation purpose. The difference in the indentation size (or shape) due to change in shape of the indenter and are shown by SPM images in Figure 1(a) to 1(f). The height and width of the indentation impressions are measured by taking the section line that passes the centre of the indentation impression. The section profiles showing the width (w) and height (h) of the

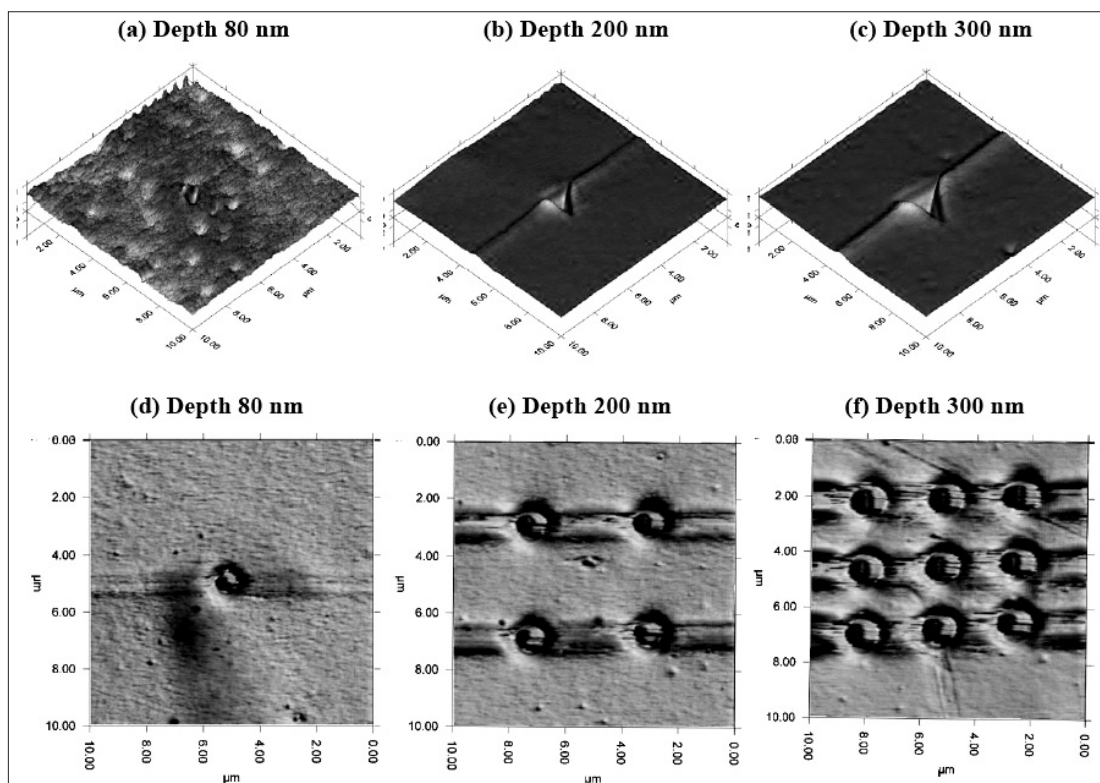


Fig. 1. Scanning probe images showing indentation impressions on the surface of the PMMA (a), (b) and (c) performed with Berkovich indenter at depths 80 nm, 200 nm and 300 nm (d), (e) and (f) performed with conical indenter at depths 80 nm, 200 nm and 300 nm.

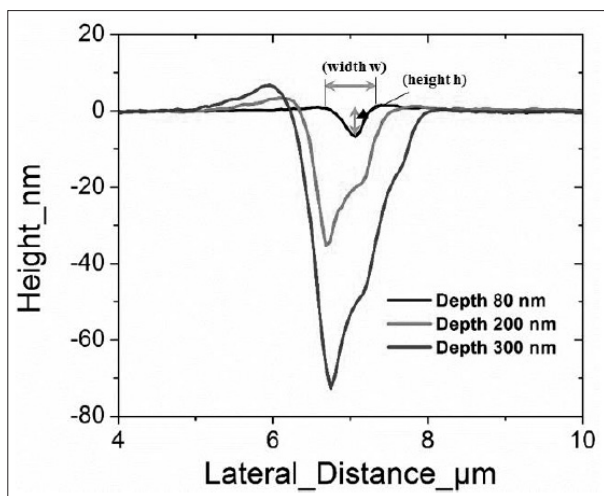


Fig. 2. Section profiles showing the width (w) and height (h) of the indentation impression.

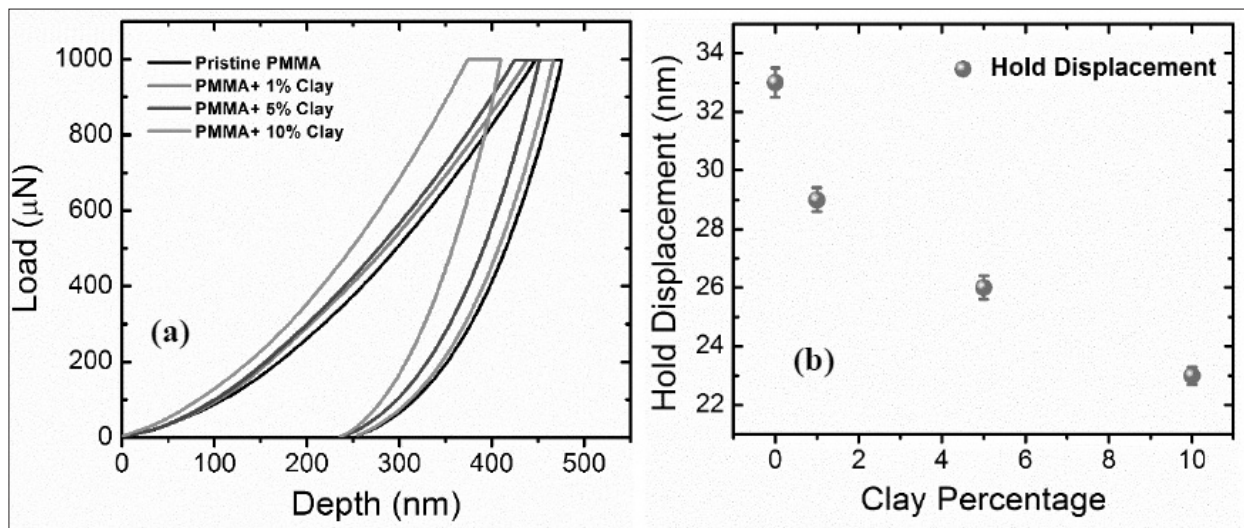


Fig. 3. Characteristic load-displacement plots showing the deviations in loading, holding and unloading curves for pristine PMMA, PMMA+1% Clay, PMMA+5% Clay and PMMA+10% Clay respectively (b) difference in hold displacement with varying clay percentage.

indentation impression is shown in Figure 2. It is seen that both width (w) and height (h) increases as the depth increases from 80 nm to 200 nm. The characteristic load-displacement plots of the material systems 1, 3, 4 and 5 are shown in Figure 2(a). It is observed as the clay concentration increases the depth of penetration decreases for the same load (i.e. 1000 μN). Different mechanical properties such as creep, Young’s modulus (Er) and hardness (H) are analysed carefully. Since the nanopillar height and width can be easily controlled by these parameters. The creep (hold displacement) is calculated from the load-displacement plot shown in Figure 3(a). The increase in the clay concentration in the polymer matrix decreases the creep behaviour which is expected.

The magnitude of pristine PMMA is around 33nm which is decreased to 22nm when clay concentration increases to 10%. The variation of Young’s modulus (Er) and hardness (H) with an increase in load are shown in Figure 4(a) and 4(b) respectively. Two interesting things are observed in these plots. Firstly, it is seen that the Er and H decreased as the load increases and reached to the constant values. Secondly, as the clay concentration increases the rise in Er and H values are observed. This increases in mechanical properties are main reason for the change in aspect ratio (i.e. ratio of height and width) of the indentation impression discussed in Figure 2. The indented samples are used to prepare soft nanopillars. The elastomer is coated on the top of the indented sample and then allowed sufficient time to cure the

elastomer. After curing, the elastomer is removed and scanned for SPM images. The scanning probe images are shown in Figure 5. From these images, it is clear that the shape of the nanopillar changes as the indenter is changed. Moreover, the height and width of the nanopillars are uniform for a given load. Apart from height and width of the nanopillar, the distance between the nanopillars can be easily controlled by choosing the appropriate gap during the indentation. The surface area without nanopillars is higher than that of the plane which will increase the bacterial adhesion in the biomedical field.

Finite element simulations are performed to validate the aspect ratio of nanopillars; however, the material considered as linear

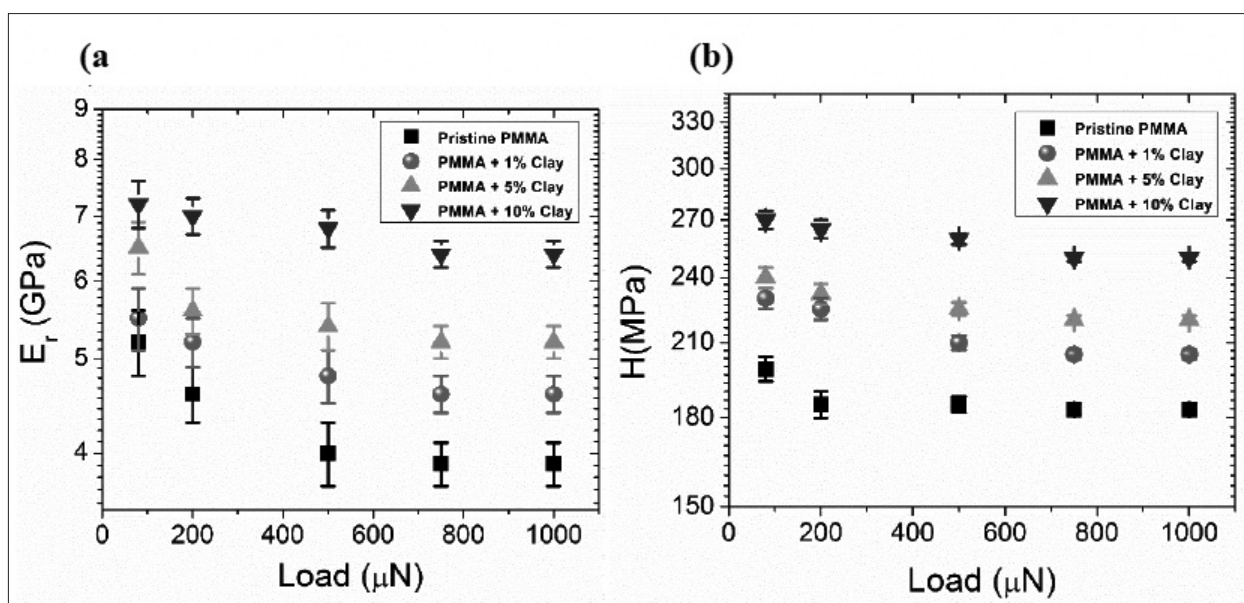


Fig. 4. Variation of measured nanomechanical properties of PMMA with increase in clay concentration and peak load (a) Young's modulus (b) Hardness.

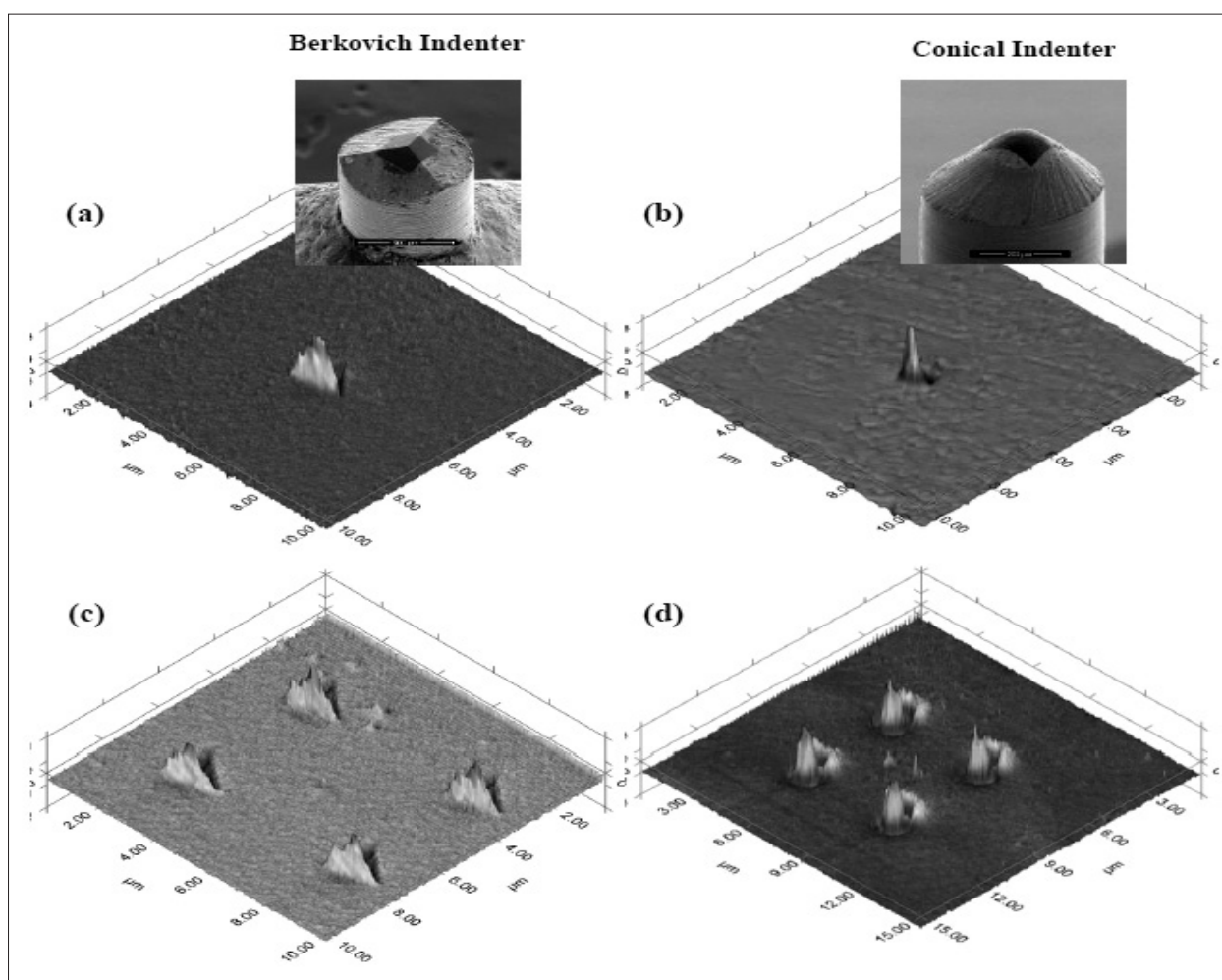


Fig. 5. Soft nano-pillar arrays of different grid sizes formed on the elastomeric substrate (a), and (c) 1 x 1, 2 x 2 grid size patterns developed using Berkovich indenter (b), and (d) 1 x 1, 2 x 2 grid size patterns developed using conical indenter.

elastic-plastic and homogenous material. High aspect ratio is observed in simulations compared to the experimental results. Since the polymer material is viscoelastic in nature as time goes, the aspect ratio changes.

4. Conclusions

Increase in mechanical properties is observed as the clay concentration increases. These changed in mechanical properties are used to control the aspect ratio of soft nanopillars. Different size soft nanopillars are successfully synthesized from the indented samples. Finite element simulations showed high aspect ratio compared to the experimental results due to the elastic-plastic nature.

References

1. Tyagi, A; Tripathi, KM; Gupta, RK: Recent Progress in Micro-scale Energy Storage Devices and Future Aspects, 'J. Mater. Chem'. A 2015, 3, 22507–22541. doi:10.1039/C5TA05666G.
2. Nguyen, BH; Nguyen, VH: Promising applications of graphene and graphene-based nanostructures, 2016.
3. Li, W; Liu, J; Zhao, D: Mesoporous materials for energy conversion and storage devices, 'Nature Reviews Materials', vol. 1, no. 6, 2016, 1 - 17. doi:10.1038/natrevmats.2016.23.
4. Moyen, E; Hama, A; Ismailova, E; Assaud, L; Malliaras, G; Hanbücken, M; Owens, RM: Nanostructured conducting polymers for stiffness controlled cell adhesion, 'Nanotechnology'. 19 Feb, 2016, vol. 27, no. 7, 074001. doi: 10.1088/0957-4484/27/7/074001. Epub 2016 Jan 21. (2016).
5. Eui, H; Suh, K: Precise tip shape transformation of nanopillars for enhanced dry adhesion, (2012) 5375–5380. doi:10.1039/c2sm07440k.
6. Sitti, M: High Aspect Ratio Polymer Micro / Nano- Structure Manufacturing using Nanoembossing, Nanomolding and Directed Self-Assembly, 'IMECE2003-42787, 2003, 293-297, <https://doi.org/10.1115/IMECE2003-42787>.
7. Lee, S; Park, B; Kim, JS; Kim, TI: Designs and processes toward high-aspect-ratio nanostructures at the deep nanoscale: unconventional nanolithography and its applications, 'Nanotechnology', vol. 27, no. 47, 2016 Nov 25, 474001.
8. Lim, JH; Leem, JW; Yu, JS: Solar power generation enhancement of dye-sensitized solar cells using hydrophobic and antireflective polymers with nanoholes, 'RSC Advances', no. 75, 2015, 61284–61289. doi:10.1039/C5RA10269C.
9. Zuiddam, MR; Frenken, JWM; Fabrication of high-aspect-ratio silicon nanopillars for tribological experiments, 2017. doi:10.1117/1.JMM.14.4.044506.
10. Chen, Ming-Hung; Chuang, Yun-Ju; Tseng, Fan-Gang: Self-masked high- aspect-ratio polymer nanopillars, 'Nanotechnology', vol. 19, no. 50, 2008, doi:10.1088/0957-4484/19/50/505301.
11. Dinesh, Chandra; Capillary Force in High Aspect-Ratio Micropillar Arrays Capillary Force in High Aspect- Ratio Micropillar Arrays, 2009.
12. Jiang, Weitao; Wang, Lanlan; Liu, Hongzhong; Ma, Haoyun; Tian, Hongmiao; Chen, Bangdao; Shi, Yongsheng; Yina, Lei; Dinga, Yucheng: Bio-inspired directional high-aspect-ratio nanopillars: fabrication and actuation, RSC Adv. no. 79, 2014, 42002–42008. doi:10.1039/C4RA05427J.
13. del Campo, Aránzazu; Arzt, Eduard: Fabrication Approaches for Generating Complex Micro- and Nanopatterns on Polymeric Surfaces, 'Chemical Reviews', ACS Publications, 49, 2008.
14. Moberlychan, WJ; Ghose, D; Arai, H; Imamura, H: Focused ion beam fabrication of spintronic nanostructures : An optimization of the milling process, 2 0 1 0 . doi:10.1088/0957- 4484/21/14/145304.
15. M. Matschuk, E. Stem, C. Toward, Injection moulding of ultra-high aspect ratio nanostructures using coated polymer tooling, (n.d.). doi:10.1088/0960-1317/24/7/075019.
16. Sedore, Matthew P: Yielding Behaviour of Electron Beam Lithography and Focused Ion Beam Made Nanocrystalline Micro / Nanopillars, Thesis (Master, Mechanical and Materials Engineering) -- Queen's University, 2016-09-30 16:22:18.869.
17. Acikgoz, Canet; Hempenius, Mark A; Huskens, Jurriaan; Vancso, G Julius: Polymers in conventional and alternative lithography for the fabrication of nanostructures, 'European Polymer Journal', vol. 47, 2011, 2033–2052. doi:10.1016/j.eurpolymj.2011.07.025.

18. Online, VA; Bae, W; Kwak, MK; Jeong, HE; Pang, C; Suh, Jeong K: *Soft Matter*, 2013, 1422– 1427. doi:10.1039/c2sm27323c.
19. Zamanzade, M; Rafael, J; Torrents, O; Motz, C; Barnoush, A: *Materials Science & Engineering A Mechanical behavior of iron aluminides: A comparison of nanoindentation, compression, and bending of micropillars*, 'Mater. Sci. Eng. A.' vol. 652, 2016, 370–376. doi:10.1016/j.msea.2015.11.088.
20. Gu, W; Loynachan, CN; Wu, Z; Zhang, Y; Srolovitz, DJ; Greer, JR: *Size-Dependent Deformation of Nanocrystalline Pt Nanopillars*, 2012. doi:10.1021/nl3036993.
21. Kumar, M; Kumar, V; Upadhyaya, P; Pugazhenti, G: *Fabrication of poly (methyl methacrylate) (PMMA) nanocomposites with modified nanoclay by melt intercalation, 'Compos. Interfaces.'* 6440(2017) 1 – 14 . doi:10.1080/15685543.2014.961780.
22. Youssef, AM; Malhat, FM; Hakim, AAA; Dekany, I: *Synthesis and utilization of poly (methylmethacrylate) nanocomposites based on modified montmorillonite*, 'Arab. J. Chem', vol. 10, 2017, 631–642. doi:10.1016/j.arabjc.2015.02.017.
23. Charitidis, CA; Koumoulos, EP: *Nanomechanical properties and nanoscale deformation of PDMS nanocomposites*, 8011(2017).doi:10.1179/1743289810Y.0000000037.
24. Ilg, P; *Stimuli-responsive hydrogels cross-linked by magnetic nanoparticles*, 'Soft Matter.', vol. 9, 2013, 3465–3468. doi:10.1039/C3SM27809C ■



Dr. Mallikarjunachari, G Presently working as a Sr. Assistant Professor in the Department of Mechanical Engineering at Madanapalle Institute of Technology & Science (MITS), Chittoor district, Andhra Pradesh. He received Ph. D. from Indian Institute of Technology Madras in the year 2016 in the Department of Applied Mechanics. He worked as a postdoctoral fellow in the Department of Chemical Engineering for two years. His area of research interest is Nanomechanics of Soft Materials. During his Ph.D. and postdoc period, he worked on different materials such as polymer thin films, interfaces, colloidal molecules, and nanocrystals. Now I am Managing, “Mechanics of Artificial Biomaterials Laboratory at MITS.

(E-mail: drmallikarjunachari@mits.ac.in)